Soot Particle Disintegration and Detection using Two Laser ELFFS

Christopher B. Stipe[1], Donald Lucas[2*], Catherine P. Koshland[3], and Robert F. Sawyer[4]

[1]Mechanical Engineering Department
Seattle University

[2]Environmental Energy Technologies Division
Lawrence Berkeley National Laboratory

[3]School of Public Health
University of California at Berkeley

[4]Mechanical Engineering Department
University of California at Berkeley

Keywords: Soot, Particles, Nanoparticles, Photofragmentation, Ablation

* Corresponding Author:

Donald Lucas
70-108B
LBNL
Berkeley, CA 94720
D_lucas@lbl.gov
510-486-7002
510-486-7303 (FAX)

Abstract

A two laser technique is used to study laser-particle interactions and the disintegration of soot by high power UV light. Two separate 20 ns laser pulses irradiate combustion generated soot nanoparticles with 193 nm photons. The first laser pulse, from 0 to 14.7 J/cm^2, photofragments the soot particles and electronically excites the liberated carbon atoms. The second laser pulse, held constant at 13 J/cm^2, irradiates the remaining particle fragments and other products of the first laser pulse. The atomic carbon fluorescence at 248 nm produced by the first laser pulse increases linearly with laser fluence from 1 to 6 J/cm^2. At higher fluences, the signal from atomic carbon signal saturates. The carbon fluorescence from the second laser pulse decreases as the fluence from the first laser increases, ultimately approaching zero as first laser fluence approaches 10 J/cm^2, suggesting that the particles fully disintegrate at high laser fluences. We use an energy balance parameter, called the photon-atom ratio (PAR), to aid in understanding laser-particle interactions. These results help define the regimes where photofragmentation fluorescence methods quantitatively measure total soot concentrations.

Introduction

Small particles from combustion adversely affect human health and contribute to climate change[1-5], leading to significant effort in developing real-time, in situ laser diagnostic techniques to detect combustion generated soot particles. In addition, recent growth in the field of nanoparticle production necessitates improved diagnostics to measure accurately the chemical composition of particles and other physical parameters, including the mean particle diameter and volume concentration.

Several measurement techniques require complete or nearly complete disintegration of particles for quantitative chemical analysis, including Laser Induced Breakdown Spectroscopy (LIBS), Aerosol Time-of-Flight Mass Spectrometry (ATOFMS), and Excimer Laser Fragmentation Fluorescence Spectroscopy (ELFFS)[6-8]. While there is substantial research on surface-laser interactions of bulk materials, the fundamental mechanisms and processes involved with methods such as laser ablation are still not well understood, and even less is known when small particles are involved.

ELFFS is a spectroscopic technique where UV photons fragment a molecule or particle and electronically excite the dissociated atomic and molecular species. The excited species emit fluorescence that is detected as a signature for the parent molecule or particle. Numerous groups have successfully used ELFFS to measure gas phase species both in the laboratory and in practical combustion systems. For example, Hartinger et al. used ELFFS to monitor sodium concentrations in the exhaust gases of a fluidized-bed coal combustor[9], and Rice et al.[10] measured sodium and potassium concentrations in the exhaust gases of a glass melting furnace. In previous work by our group, we used ELFFS to measure gas phase species such as chlorinated hydrocarbons, toxic metals, and ammonia[11-15].

The ELFFS technique is concurrently being developed to measure nanoparticles; however, fundamental questions remain concerning the laser-particle interactions that lead to particle disintegration. The resulting fluorescence signal depends both on the chemical and physical composition of the irradiated particles and the laser fluence, but to what extent is unknown. Nunez et al.[16,17] measured various sodium containing aerosols with ELFFS, including NaCl, NaOH, and Na_2SO_4, detecting emission from sodium as the signature. To study the particle disintegration and dependence of the sodium signal on the composition of the original particle, time-resolved sodium emission was collected. By comparing the ELFFS measurements of NaCl, NaOH, and Na_2SO_4 particles, they determined the time to reach the peak fluorescence signal depended on the chemical composition of the particle. They attributed the variation in rise time of the fluorescence signal to the disintegration of the particle, which strongly depends on the primary energy deposition step. Only the fluorescence signal for NaCl, which has the lowest enthalpy of vaporization of the three particles studied, saturated at high laser fluences, suggesting the NaOH and Na_2SO_4 particle did not absorb sufficient energy for full disintegration. The unknown extent of particle disintegration hinders the analytical capability of the technique.

In our laboratory, we developed ELFFS to detect numerous nanoparticles, including lead, ammonium sulfate and nitrate, and combustion generated soot particles[18-20], but the physical parameter measured by ELFFS remains uncertain. When measuring ammonium sulfate and nitrate particles, the fluorescence signal was proportional to the surface area of the particles.

When measuring soot particles, the fluorescence signal was proportional to the volume concentration of the particles.

In this study, a two laser ELFFS technique is employed to study laser-particle interactions leading to particle disintegration and gas phase species excitation. Two different 20 ns 193 nm laser pulses irradiate the soot particles and electronically excite carbon atoms, which then fluoresce at 248 nm. The time separation between the first and second laser pulses is long enough to allow the excited atoms from the first pulse to fluoresce, but short enough to freeze the flow field between pulses. The threshold for complete particle disintegration is explored, and spectroscopic evidence provides insight into the dominant disintegration mechanism.

Experimental Apparatus

Figure 1 shows the experimental apparatus for the two laser photofragmentation of soot particles. Combustion generated particles are created by an inverted, co-flow, non-premixed burner[21]. Methane flows at 1.43 liters per minute (lpm) through a center jet surrounded by a shroud of 19 lpm of co-flow air enclosed in a 5 cm diameter quartz tube. Air injected 4 cm downstream of the flame tip at 25 lpm immediately dilutes and cools the soot and exhaust gases exiting the quartz tube. The soot and exhaust gases then flow through a 140 cm stainless steel tube to ensure uniform mixing. An ejector pump extracts 2.5 lpm of flow from the stainless steel tube through diffusion dryer to remove the water generated by the flame and through a diffusion denuder to remove unburned gas phase hydrocarbons. Air driving the ejector pump dilutes the extracted flow by 8:1. Of the 20 lpm exiting the ejector pump, 6.5 lpm flows to the laser interrogation region, and the remaining 12.5 lpm flows to a waste exhaust ventilation hood.

A Scanning Mobility Particle Sizing (SMPS) system, consisting of a Differential Mobility Analyzer (DMA) (TSI model 3071A) and a Condensation Particle Counter (CPC) (TSI model 3025A), measures the electric mobility diameter and number concentration of the particles. This system was described in detail previously[21].

A Lambda Physik LPX210i ArF excimer laser produces the first laser pulse. A 38.1 mm diameter, 203 mm focal length, plano-convex lens focuses the beam to a spot size of 0.41 by 1.14 mm, or $4.6 \cdot 10^{-3}$ cm^2. A Lambda Physik EMG 102 ArF excimer laser produces the second 20 ns pulse of 193 nm photons. The second beam is redirected by two 90°, 50.8 mm diameter UV grade mirrors to ultimately coincide with the first beam, while traveling in the opposite direction. A 38.1 mm diameter, 203 mm focal length, plano-convex lens focuses the second beam to a spot size of 0.31 by 0.96 mm, or $2.9 \cdot 10^{-3}$ cm^2. The second beam has a smaller cross-sectional area in the interrogation region to ensure that it only measures particles illuminated by the first laser. The focused beams are aligned by ablating a hole through a piece of paper with the first laser and then centering the second beam in that hole.

The particle-laden flow travels through a 0.9 cm diameter nozzle at 200 cm/s into the laser interrogation region. The residence time of the particles in the laser interrogation region is 0.2 ms. The time between pulses varies from 100 ns to 1 μs, so the flow is essentially frozen between the two pulses. The laser repetition rate of 10 Hz is slow enough for the probe volume to clear between subsequent first laser shots.

We collect fluorescence at a right angle to the laser beams. A 50.8 mm, 49 mm focal length bi-convex lens focuses a fraction of the isotropically emitted fluorescence into a 0.3 m monochromator (McPherson 218). The slitwidths of the monochromator are 0.4 mm, which produces a spectral resolution of 1 nm. A photomultiplier (Hamamatsu R928) detects the photons. The signal is not gated, and we use the peak fluorescence in a 100 ns window around the laser pulse.

Photon-Atom Ratio (PAR)

The extent of particle disintegration by laser irradiation depends on the energy absorbed by the particle and the energy required to break the chemical bonds of the particle. The energy absorbed is a function of the laser fluence and cross-sectional area of the particles, while the energy required to disintegrate a particle is a function of the enthalpy of atomization. In the literature, signals are often plotted against laser energy or fluence[16,18]. While this metric is adequate for

comparing results of monodisperse particle distributions or when irradiating a bulk surface, it is not adequate for comparing measurements of particles with different size distributions. The surface area to volume ratio directly affects the energy absorbed and the energy required to disintegrate the particles. Thus, another parameter is needed when polydisperse distributions are compared.

A more descriptive parameter, called the photon/atom ratio or PAR, allows for comparisons of different particle size distributions. PAR is the ratio of the number of photons striking the particle to the number of atoms in the particle. The number of photons striking the particle is calculated from the laser fluence and the total cross-sectional area of the soot particles, while the number of atoms is determined using the volume and density of the particles. While the PAR number is not a fundamental property, it is a useful parameter for photon-particle interactions. For example, a PAR number of unity occurs when one photon is incident on a particle surface for each atom contained in the particle. For photons with the same energy as the average bond energy in a particle, the PAR number must be unity or higher for complete disintegration of the particle. Note that the fluence alone is not as useful for comparing results of systems of different particle size distributions, as the incident energy to volume ratio of the particles is not constant.

The PAR concept for particles can be extended with adjustments for the absorption coefficient of the particle material, the enthalpy of atomization, the excitation energy, and the photon energy. For soot irradiated by 193 nm photons, the energy in one photon is larger than a typical in-plane carbon-carbon sigma bond in graphite (620 vs. 524 kJ/mole), so each photon can break at least one bond. The energy necessary to fully convert graphite to carbon atoms is 716 kJ/mole. These values serve only as a guide as the actual atomization energy of soot strongly depends on it complex chemical structure.

Results

The combustion generated soot particles in this study have a mean electric mobility diameter of 280 nm, a number concentration of $9.2 \cdot 10^{5}$ cm^{-3}, and a volume concentration of $2.3 \cdot 10^{12}$

nm^3/cm^3, as measured by the SMPS. If fully disintegrated to carbon atoms, the concentration in air is 9.4 ppm.

Carbon atom emission from the $^1P_1^0$ to $^1S_0$ transition is measured at 248 nm [22]. A Schumann-Runge O_2 transition at 250 nm[23] partially overlaps the atomic carbon fluorescence at 248 nm, and is subtracted from the carbon atom signal. Photofragmented CO_2 can also yield a 248 nm carbon atom signal, but when the fluence is below 16 J/cm^2 this peak is negligible for the 0.5% CO_2 concentrations in the diluted exhaust. Interestingly, no long lifetime, broadband emission associated with either LII or plasma formation is observed for the conditions studied. In LII studies, the low wavelength tail of the blackbody emission is generally observed from 300 to 1000 nm, depending on the soot temperature[24]. We have observed LII in our system when a 532 nm Nd:YAG laser at a similar fluence replaced the 193 nm source, and a plasma was observed when using 193 nm light to ablate and/or fragment a solid surface containing lead[25]. The signal from 193 nm photons scattered from the particles is too small to use as a quantitative measure of particle disintegration. In addition, the scattered signal is not easily interpreted; changes in the signal are difficult to ascribe to changes in morphology or particle size and mass[26].

Figure 2 shows the dependence of the atomic carbon fluorescence signal on the laser fluence or PAR. Each point is a 100 shot average of the peak fluorescence centered at 248 nm. The carbon fluorescence generated by the first laser pulse, which varies from 0 to 14.7 J/cm^2 (PAR of 0 to 4.5), has three distinct regions: a threshold, a linear region, and saturation. The fluorescence signal is linearly proportional to the fluence from 1 to 6 J/cm^2, with a threshold at approximately 1 J/cm^2. Above 6 J/cm^2, the slope of the curve becomes less steep, with apparent saturation near 10 J/cm^2. Results from the second laser, fired at a constant 13 J/cm^2, are also shown in Fig. 2. Note that the second pulse fluence is large enough to saturate the signal if irradiating the original particles.

Two different delay times (100 ns and 1 μs) between the first and second laser pulses were studied. For both delay times, the fluorescence from the second laser pulse is a maximum when firing on a “fresh” volume of particles not previously irradiated by the first laser (plotted at a laser fluence of zero in Fig. 2). Note that the second laser signal maximum is 65% of the signal

as the first laser at the same fluence (13 J/cm^2) because the probe volume of the second laser is smaller by the same fraction. In both the 1 μs and 100 ns delay cases, the fluorescence signal from the second laser pulse decreases as the PAR number from the first laser increases, but the 100 ns delay has a less steep slope. Interestingly, for the same first laser fluence, the carbon fluorescence from the second laser pulse is larger at 100 ns than at a 1 μs separation time, which was the basis for the following directed study.

Figure 3 illustrates the effect of time separation between the laser pulses on the atomic carbon fluorescence from the second laser pulse. The fluences for the first and second lasers are 3.8 and 13 J/cm^2, respectively. The PAR for the first laser is approximately 1. The fluorescence signal decreases rapidly within the first 500 ns (the laser pulse is approximately 20 ns). The signal then remains constant until the probe volume begins to refill, resulting in a linear increase in the signal when the pulse separation increases from 10 to 200 μs (not shown in the figure).

Discussion

Effects of the First Laser Pulse

The results presented in Fig 2. have several distinctive features: there is a threshold for observing emission at 248 nm, the signal increases linearly from 1 to 6 J/cm^2, and the signal begins to show saturation behavior above 6 J/cm^2. A threshold for fluorescence appears at 1 J/cm^2 or a PAR of 0.3. We previously observed a threshold near 1 J/cm^2 when irradiating soot produced by a diesel engine[27]. Also, particles of other chemical compositions have a fluorescence threshold. Nunez and Omenetto[16] observed a threshold for sodium emission when photofragmenting NaCl, NaOH, and Na_2SO_4 particles. The threshold increased in the following order: NaCl < NaOH < Na_2SO_4. The authors associated the threshold to the energy required to melt and vaporize the particles, which are mechanisms that are probably not important here since the disintegration is most likely dominated by photodissociation and not heating and vaporization. Interestingly, Mechler[28] observed a threshold for plasma formation and the ejection of carbon from a bulk graphite surface by 193 nm laser ablation at a similar fluence of approximately 1 J/cm^2. In our system, no optical evidence for a plasma was observed even at fluences an order of magnitude larger than

those used in the Mechler study, suggesting that the laser interaction with nanoscale particles differs from a bulk material. It should also be noted that we and other researchers observe no obvious thresholds for numerous gas phase molecules studied with ELFFS[29].

In other experiments conducted in our laboratory[30], significant changes in the particle size distribution were observed when irradiating soot particles at fluences below the observed fluorescence threshold of 1 J/cm^2 (PAR of 0.15), revealing that the laser affects the particles even in the absence of detectable carbon atom fluorescence. These previous experiments also showed that the volume concentration in the laser interrogation region does not change at PARs below 0.15. At higher PARs, there is a measurable loss of volume, presumably through the oxidation of the photodissociated gas phase carbon atoms. Here, the threshold is likely due to the production of only a small amount of excited gas phase carbon and not caused by the melting and vaporization of the particle. Our results can be compared to those of Srinivasan et al.[31,32] who performed 193 and 248 nm laser ablation studies on poly(methyl metacrylate). They found a threshold at approximately 0.7 J/cm^2 for rapid etching, but a small amount was ablated even at lower fluence. Solid phase material ejected from the surface showed no sign of significant heating.

Above the threshold value, the fluorescence signal at 248 nm increases linearly from 1 to 6 J/cm^2, corresponding to PARs from 0.3 to 1.8. Linear behavior is common for ELFFS and other sequential multiphoton processes, where a rate limiting step is usually saturated. Above 6 J/cm^2, or a PAR of approximately 2, the atomic carbon fluorescence begins to saturate. Damm et al.[27] also observed a saturation of the ELFFS fluorescence signal of diesel particles, and Nunez et al.[16] observed a saturated signal for NaCl particles. In the saturated region, either the laser pulse fully atomizes the particles or radiation trapping becomes significant. Previous results in our laboratory showed that the atomic carbon fluorescence signal is linearly proportional to the volume concentration of the soot particles when irradiated in the saturated fluorescence regime, and that radiation trapping is not important[6].

The atomic carbon fluorescence saturates near a PAR of 2, evidence that the ELFFS process efficiently atomizes the particles and excites the liberated species. The conversion efficiency

here can be compared with that of LIBS. In a study determining the largest diameter of a particle disintegrated by LIBS, Carranza and Hahn[33] found that approximately 10^5 more energy exists in the plasma than necessary to completely atomize a 2 μm particle (PAR for the Carranza and Hahn study is on the order of 1500). They concluded that the photon energy does not directly disintegrate the particle, but that the energy in the laser induced plasma conducts to the particle, causing thermal vaporization. As excessive energy deposits at the surface of the particle, forming a plasma, the remaining incident photons are absorbed by the plasma and not the particle itself. With ELFFS, a plasma does not form, so it may thus be possible to fully disintegrate larger particles. The upper size limit is not known, however, as it is difficult to predict where plasma formation will begin.

Two Laser Experiments

In Fig. 2, the carbon atom fluorescence from the second laser pulse firing 1 μs after the first pulse decreases rapidly as the fluence of the first pulse increases. The fluence of the second pulse is 13 J/cm^2, corresponding to a PAR of 4 if irradiating "fresh" particles. Thus, the second pulse has sufficient energy to fully disintegrate the particle fragments and molecules remaining after the first pulse.

The fluorescence signal at 248 nm produced by the second laser pulse can be attributed to the photodissociation and/or excitation from the remaining particles, particle fragments, molecular species, and atomic species generated by the first laser pulse. Fluorescence at 248 nm is from carbon atoms excited from the $^1D_2$ state, which absorb a 193 nm photon. The $^1D_2$ state is populated during the photofragmentation of a soot particle or carbon containing molecule. The $^1D_2$ state is not populated thermally, since the lack of incandescence or plasma emission precludes high temperature regions around the particles. Thus, none of the carbon atoms produced in or quenched to the $^3P_{0,1,2}$ ground state contribute to the fluorescence at 248 nm by single photon absorption. Carbon atoms in the $^3P_{0,1,2}$ could simultaneously absorb two photons, ionize, relax to the $^1P_1{}^0$ state, and then emit at 248 nm; however, the fluences used here do not produce a significant population of ionized species. In addition, atomic carbon remaining after

the first laser pulse does not directly contribute to the second laser pulse signal because it will be quenched or oxidized during the 1 μs between laser pulses.

The highest first laser pulse fluence (14.7 J/cm^2) does not produce significant atomic carbon fluorescence from CO or CO_2 in the exhaust gas[22]. The second laser pulse, at 13 J/cm^2, also will not produce fluorescence from these species since the amount produced by oxidiation of reactive carbon species is small. However, the second laser pulse can measure remaining particle fragments, carbon containing molecules not oxidized between pulses, and any carbon that recombines with remaining particles or molecules.

The signal from the second laser pulse approaches zero as the first laser pulse saturates, indicating that the majority of the carbon atoms ejected by the first laser pulse do not recondense to particles or fragmentable molecules. This result is expected, since as the first laser pulse fluorescence saturates, most of the original particles disintegrate, leaving no photofragmentable species for the second laser pulse. Particles can be produced by laser ablation of a bulk material, but this nucleation generally require 50 μs or longer[34,35], so the second laser pulse will not detect any new particles formed between the pulses. The fluorescence signal from the second laser pulse at a time separation of 100 ns also tends towards zero, but with a lower slope. The fluorescence signal at 100 ns is larger than that for 1 μs for all conditions, except at the highest first laser pulse fluence where they are similar.

Figure 3 shows a strong dependence of the fluorescence signal from the second laser pulse on the time separation between pulses. The PAR for the first pulse is approximately 1 (3.8 J/cm^2), where about half of the particles remain after photofragmentation, as seen in Fig. 2. The second pulse fluence is high enough to saturate the fluorescence signal when firing on “fresh” particles (13 J/cm^2), so we expect the second pulse to measure the remaining particle volume. At the shortest time delay of 100 ns, approximately 30% of the original carbon atoms are not measured by the second laser. Delay times of less than 100 ns could not be obtained consistently because there is a relatively large triggering jitter present in firing the excimer lasers. From 100 to 500 ns, the signal decreases linearly to about half of its original value, in good agreement with the single laser results, where the signal is half that of the saturated value obtained at the highest fluences.

Fluorescence from the second laser pulse remains constant from 500 ns to 10 μs, where it begins to increase due to new particles entering the laser probe volume. The constant signal implies all reactive species are oxidized, the atoms in the $^1D_2$ state are fully quenched, particle disintegration has terminated, and condensation is not significant. If the reduction in signal from 100 to 500 ns is due to oxidation of gas phase species or quenching, which is discussed in detail below, then the second laser pulse can be assumed not to measure carbon atoms already measured by the first pulse, making two laser ELFFS a powerful tool for determining the extent of particle disintegration.

Two potential mechanisms converting measurable carbon species to nondetectable species between laser pulses are the oxidation of carbon atoms or other carbon species and the quenching of carbon atoms in the $^1D_2$ state to the ground state. Oxygen atoms, produced by the photolysis of oxygen molecules with 193 nm light, could react with the particles even if no gas phase carbon species were produced. While the concentration of O atoms produced by the first laser pulse is roughly equal to the concentration of carbon atoms in the particle laden gas stream, the time necessary for oxidation to occur is much longer than the times observed experimentally. Oxygen molecules, at a concentration approximately 10^4 times that of the carbon atoms in the laser probe volume, probably do react with carbon atoms or other reactive fragments such as C_2. While the rates for some of these reactions are known, it is difficult to model the system as the products from the fragmentation process are not well characterized.

Another possibility for the signal loss illustrated in Fig. 3 is the existence of carbon atoms in the $^1D_2$ state. A fraction of the carbon excited to the $^1P_1{}^0$ state fluoresce at 193 nm, returning to the $^1D_2$ state. Atoms remaining in this state could contribute to the fluorescence at 248 nm if re-excited to the $^1P_1{}^0$ state by the second laser pulse. The transition from the $^1D_2$ state to the ground $^3P_{1,2,3}$ state is forbidden, making the lifetime of the $^1D_2$ state long, and little is known about the reactions from this state. Quenching of these atoms would reduce the fluorescence signal over time. However, if this mechanism were dominant, then increasing the first laser fluence (and the amount of carbon in the $^1D_2$ state) should lead to a larger signal from the second laser at a fixed time separation, assuming the same relaxation time. This was not the observed behavior.

Dyer and Srinivassan[32] measured the stress waves generated by the interaction of 193 nm photons with polyvinyylidenefluoride films. They found that ablation begins in a few nanoseconds, lasts only slightly longer than the laser pulse, and that heating was not the mechanism responsible for mass loss. Applied to our results, this suggests that the changes in the first 100 ns are due to direct photofragmentation of the particles. Since we also did not observe incandescence, heating is not the cause of our mass loss. This leaves oxidation of the particle by oxygen atoms or ozone produced by the laser as the likely mechanism for particle loss at times longer than 100 ns.

Conclusions

Two laser ELFFS using 193 nm light is used to study the interaction of UV photons with combustion generated soot particles. This study provides evidence that the particles are fully disintegrated when the first laser pulse fluorescence signal is saturated. The full disintegration is confirmed by the second pulse fluorescence tending towards zero as the first pulse fluorescence saturates. In the saturated regime, the fluorescence is thus independent of the laser fluence and proportional to the volume concentration of the particles in the probe volume. At the experimental conditions employed, neither incandescence nor plasma formation is observed. 193 nm photons are effectively converted to the production of gas phase species that can be measured by fluorescence.

A non-dimensional parameter, the photo/atom ratio, is introduced to explore aspects of the photon-particle interactions and provide an upper limit on particle atomization. Atomic carbon fluorescence monitored at 248 nm from the first laser pulse is linearly proportional to the PAR number from 0.3 to 2 (1 to 6 J/cm^2). Near a PAR value of 2, the signal begins to saturate. Disintegration and excitation of remaining particle fragments and non-oxidized carbon containing molecules produce a majority of the second laser pulse signal. The second pulse signal tends towards zero as the atomic carbon signal from the first laser saturates, confirming that the particle is completely disintegrated. The atomic carbon signal from the second pulse decreases as the time separation between pulses increases up to 500 ns. At longer delay times the second pulse measures particles not fully disintegrated by the first pulse.

Acknowledgements

We thank Jong Hyun Choi for his suggestions and discussions. This work was supported by the Environmental Health Sciences Superfund Basic Research Program (Grant Number P42ESO47050-01) from the National Institute of Environmental Health Sciences, NIH, with funding provided by the EPA and the Toxic Substances Research and Teaching Program. Its contents are solely the responsibility of the authors and do not necessarily represent the official views of NIEHS, NIH, or EPA.

References

[1] C. P. Koshland and S. L. Fischer, "Diagnostic Requirements for Toxic Emission Control," in *Applied Combustion Diagnostics*, K. Kohse-Hoinghaus and J. B. Jefferies, eds. (Taylor and Francis, New York, 2002), pp. 606-626.

[2] D. W. Dockery, C. A. Pope, X. Xu, J. D. Spengler, J. H. Ware, M. E. Fay, B. G. Ferris, and F. E. Speizer, "An Association Between Air Pollution and Mortality in Six U.S. Cities," New Engl. J. Med. **329,** 1753-1759 (1993).

[3] A. Peters, D. W. Dockery, J. E. Muller, and M. A. Mittleman, "Increased Particulate Air Pollution and the Triggering of Myocardial Infarction," Circulation, Am. Heart Assoc. **103,** 2810-2815 (2000).

[4] M. Z. Jacobson, "Strong Radiative Heating Due to the Mixing State of Carbon Black in Atmospheric Aerosols," Nature **409,** 695-697 (2001).

[5] J. T. Houghton, Y. Ding, D. J. Griggs, M. Noguer, P. J. van der Linden, X. Dai, K. Mashell, and C. A. Johnson, “Climate Change 2001: The Scientific Basis: Contribution of Working Group I to the Third Assessment Report of the Intergovernmental Panel on Climate Change,” IPCC Report, (Cambridge, UK 2001).

[6] C. B. Stipe, B. S. Higgins, D. Lucas, C. P. Koshland, and R. F. Sawyer,"Soot Detection Using Excimer Laser Fragmentation Fluorescence Spectroscopy," Proc. Combust. Instit. **29,** 2759-2766 (2002).

[7] M. Z. Martin, M. D. Cheng, and R. C. Martin, "Aerosol Measurement by Laser-Induced Plasma Technique: A Review," Aerosol Sci. Technol. **31,** 409-421 (1999).

[8] K. A. Prather, T. Nordmeyer, and K. Salt, "Real-Time Characteriztion of Individual Aerosol Particles Using Time-of-Flight Mass Spectrometry," Anal. Chem. **66,** 1403-1407 (1994).

[9] K. T. Hartinger, P. B. Monkhouse, J. Wolfrum, H. Baumann, and B. Bonn, "Determination of Flue Gas Alkali Concentrations in Fluidized-Bed Coal Combustion by Excimer-Laser-Induced Fragmentation Fluorescence," Proc. Combust. Instit. **25,** 193-199 (1994).

[10] S. Rice, D. Morrison, M. Velez, and J. Almanza, “NaOH Concentration in Furnace Offgas Measured by Laser-Induced Fragmentation Fluorescence,” Sandia Report, Vol. 23, No. 3 (2002).

[11] C. S. McEnally, R. F. Sawyer, C. P. Koshland, and D. Lucas, "Sensitive In Situ Detection of Chlorinated Hydrocarbons in Gas Mixtures," Appl. Opt. **33,** 3977-3984 (1994).

[12] C. S. McEnally, R. F. Sawyer, C. P. Koshland, and D. Lucas, "In Situ Detection of Hazardous Waste," Proc. Combust. Inst. **25,** 325-331 (1994).

[13] S. G. Buckley, C. S. McEnally, R. F. Sawyer, C. P. Koshland, and D. Lucas, "Metal Emissions Monitoring Using Excimer Laser Fragmentation Fluorescence Spectroscopy," Combust. Sci. Technol. **118,** 169-188 (1996).

[14] S. G. Buckley, C. P. Koshland, R. F. Sawyer, and D. Lucas, "A Real-time Monitor for Toxic Metal Emissions from Combustion Systems," Proc. Combust. Instit. **26,** 2455 (1996).

[15] S. G. Buckley, C. J. Damm, W. M. Vitovec, L. A. Sgro, R. F. Sawyer, C. P. Koshland, and D. Lucas, "Ammonia Detection and Monitoring with Photofragmentation Fluorescence," Appl. Opt. **37,** 8382-8391 (1998).

[16] M. H. Nunez and N. Omenetto, "Experimental Investigation of Sodium Emission Following Laser Photofragmentation of Different Sodium-Containing Aerosols," Appl. Spectrosc. **55,** 809-815 (2001).

[17] M. H. Nunez, P. Cavalli, G. Petrucci, and N. Omenetto, "Analysis of Sulfuric Acid Aerosols by Laser-Induced Breakdown Spectroscopy and Laser-Induced Photofragmentation," Appl. Spectrosc. **54,** 1805-1816 (2000).

[18] S. G. Buckley, R. F. Sawyer, C. P. Koshland, and D. Lucas, "Measurements of Lead Vapor and Particulate in Flames and Post-flame Gases," Combust. And Flame **128,** 435-446 (2002).

[19] C. J. Damm, D. Lucas, R. F. Sawyer, and C. P. Koshland, "Excimer Laser Fragmentation Fluorescence Spectroscopy as a Method for Monitoring Ammonium Nitrate and Ammonium Sulfate Particles," Chemosphere **42,** 655-661 (2001).

[20] C. J. Damm, D. Lucas, R. F. Sawyer, and C. P. Koshland, "Real-Time Measurement of Combustion Generated Particles with Photofragmentation-Fluorescence," Appl. Spectrosc. **55,** 1478-1482 (2001).

[21] C. B. Stipe, B. S. Higgins, D. Lucas, C. P. Koshland, and R. F. Sawyer, "An Inverted Co-Flow Diffusion Flame for Producing Soot," Rev. Sci Instr. (to be published).

[22] R. C. Sausa, A. J. Alfano, and A. W. Miziolek, "Efficient ArF Laser Production and Detection of Carbon Atoms from Simple Hydrocarbons," Appl. Opt. **26,** 3588-3593 (1987).

[23] M. P. Lee and R. K. Hanson, "Calculations of O2 Absorption and Fluorescence at Elevated Temperatures for a Broadband Argon-Fluoride Laser Source at 193nm," J. Quant. Spectrosc. Radiat. Transfer **36,** 425-440 (1986).

[24] R. Vander Wal, "Laser-Induced Incandescence: Detection Issues," Appl. Opt. **35,** 6548-6559 (1996).

[25] J. H. Choi, C. J. Damm, N. J. O'Donovan, R. F. Sawyer, C. P. Koshland, and D. Lucas, "Detection of Lead in Soil with Excimer Laser Fragmentation Fluorescence Spectroscopy (ELFFS)," Appl. Spectrosc. **59** (2005).

[26] M. F. Modest, "*Radiative Heat Transfer,"* 1st ed. (McGraw-Hill, New York, 1993).

[27] C. J. Damm, D. Lucas, R. F. Sawyer, and C. P. Koshland, "Characterization of Diesel Particulate Matter With Excimer Laser Fragmentation Fluorescence," Proc. Combust. Instit. **29**, 2767-2774 (2002).

[28] A. Mechler, P. Heszler, Z. Marton, M. Kovacs, T. Szorenyi, and Z. Bor, "Raman Spectroscopic and Atomic Force Microscopic Study of Graphite Ablation at 193 and 248 nm," Appl. Surf. Sci. **154-155,** 22-28 (2000).

[29] J. B. Simeonsson and R. C. Sausa, "A Critical Review of Laser Photofragmentation Fragment Detection Techniques for Gas Phase Chemical Analysis," Appl. Spectrosc. Rev. **31,** 1-72 (1996).

[30] C. B. Stipe, J. H. Choi, D. Lucas, C. P. Koshland, and R. F. Sawyer, "Nanoparticle Production by UV Irradiation of Combustion Generated Soot," J. Nanoparticle Res. (to be published).

[31] R. Srininvasan, B. Braren, D. E. Seeger, and W. Dreyfus, "Photochemical Cleavage of a Polymeric Solid: Details of the Ultraviolet Laser Ablation of Poly(methyl methacrylate) at 193 and 248 nm," Macromolecules **19,** 916-921 (1986).

[32] P. E. Dyer and R. Srininvasan, "Nanosecond Photoacoustic Studies on Ultraviolet Laser Ablation of Organic Polymers," Appl. Phys. Lett. **48,** 445-447 (1986).

[33] J. E. Carranza and D. W. Hahn, "Assessment of the Upper Particle Size Limit for Quantitative Analysis of Aerosols Using Laser-Induced Breakdown Spectroscopy," Anal. Chem. **74,** 5450-5454 (2002).

[34] D. B. Geohegan, A. A. Puretzky, G. Duscher, and S. J. Pennycook, "Time-Resolved Imaging of Gas Phase Nanoparticle Synthesis by Laser Ablation," Appl. Phys. Lett. **72,** 2987-2989 (1998).

[35] E. A. Rohlfing, "Optical Emission Studies of Atomic, Molecular, and Particulate Carbon Produced from a Laser Vaporization Cluster Source," J. Chem. Phys. **89,** 6103 (1988).

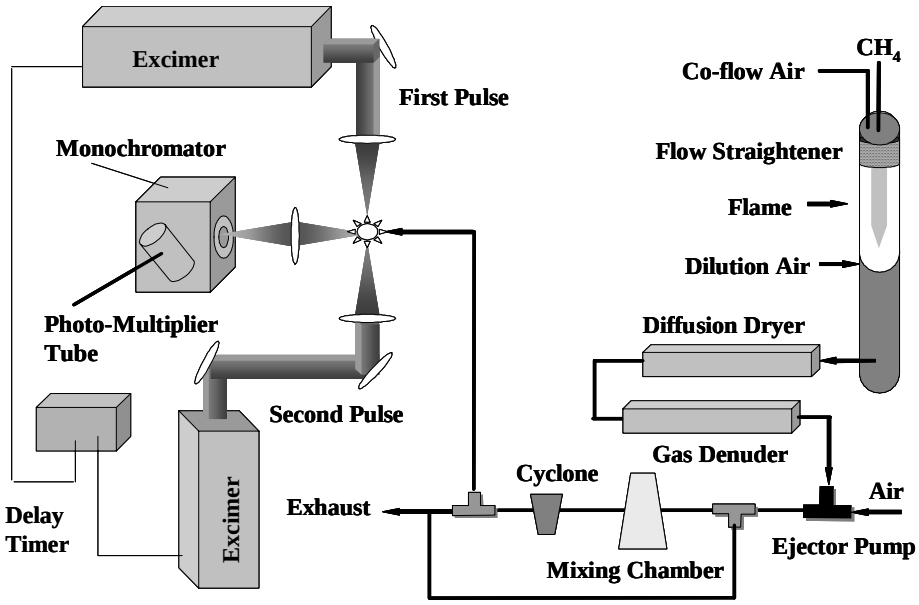
Excimer
First Pulse
Monochromator
Photo-Multiplier Tube
Second Pulse
Delay Timer
Excimer
Exhaust
Cyclone
Mixing Chamber
Ejector Pump
Air
Gas Denuder
Diffusion Dryer
Dilution Air
Flame
Flow Straightener
Co-flow Air
CH4

Figure 1

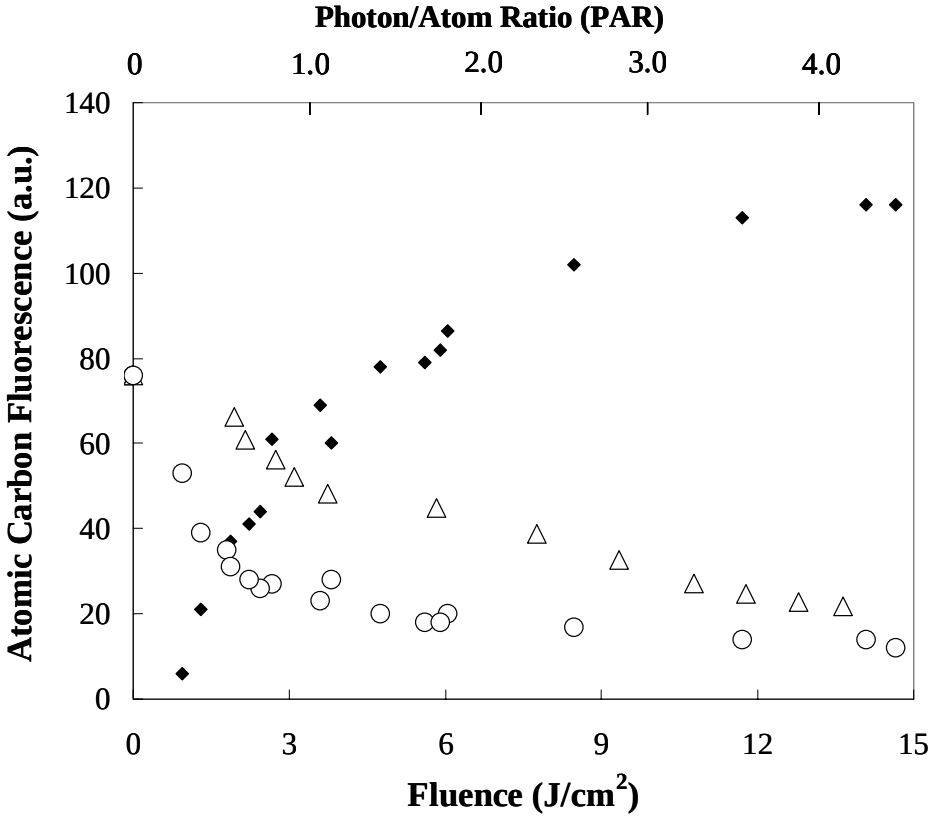
Photon/Atom Ratio (PAR)
0
1.0
2.0
3.0
4.0
Atomic Carbon Fluorescence (a.u.)
140
120
100
80
60
40
20
0
0
3
6
9
12
15
Fluence (J/cm2)

Figure 2

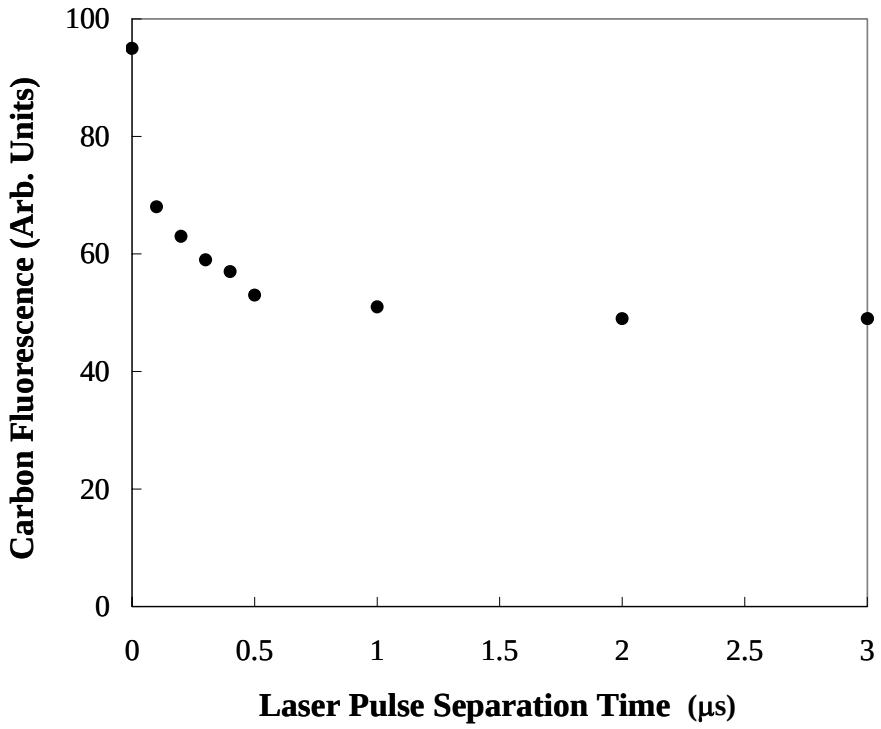
Carbon Fluorescence (Arb. Units)
100
80
60
40
20
0
0
0.5
1
1.5
2
2.5
3
Laser Pulse Separation Time (μs)

Figure 3

Figure Captions

Figure 1: Experimental Apparatus

Figure 2: Two laser fragmentation by 193 nm photons of soot particles in air. The atomic carbon fluorescence produced by the first laser is shown in black diamonds, and the fluorescence produced by the second pulse is shown as open circles (1 μs) and open triangles (100 ns). The fluence of the first pulse varies from 0 to 14.7 J/cm^2, while the second pulse is constant at 13 J/cm^2. These data are 100 shot averages taken at a laser repetition rate of 10 Hz.

Figure 3: Carbon fluorescence from the second laser pulse as a function of pulse separation time from 0 to 3 μs. The decrease in signal between laser pulses is likely due to oxidation of atomic carbon, carbon molecules, and soot particles remaining after the first laser pulse. The signal remains constant from 1 to 10 μs.